Published in final edited form as:
Neuroimage. 2013 December ; 83: . doi:10.1016/j.neuroimage.2013.07.068.

Diffusion MRI of the Developing Cerebral Cortical Gray Matter can be Used to Detect Abnormalities in Tissue Microstructure Associated with Fetal Ethanol Exposure

Lindsey A. Leigland[1,2], **Matthew D. Budde**[3], **Anda Cornea**[4], and **Christopher D. Kroenke**[1,2,4,*]

[1]Department of Behavioral Neuroscience, Oregon Health & Science University, Portland, OR

[2]Advanced Imaging Research Center, Oregon Health & Science University, Portland, OR

[3]Department of Neurosurgery, Medical College of Wisconsin, Milwaukee, WI

[4]Oregon National Primate Research Center, Oregon Health & Science University, Portland, OR

Abstract

Fetal alcohol spectrum disorders (FASDs) comprise a wide range of neurological deficits that result from fetal exposure to ethanol (EtOH), and are the leading cause of environmentally related birth defects and mental retardation in the western world. One aspect of diagnostic and therapeutic intervention strategies that could substantially improve our ability to combat this significant problem would be to facilitate earlier detection of the disorders within individuals. Light microscopy-based investigations performed by several laboratories have previously shown that morphological development of neurons within the early-developing cerebral cortex is abnormal within the brains of animals exposed to EtOH during fetal development. We and others have recently demonstrated that diffusion MRI can be of utility for detecting abnormal cellular morphological development in the developing cerebral cortex. We therefore assessed whether diffusion tensor imaging (DTI) could be used to distinguish the developing cerebral cortices of ex vivo rat pup brains born from dams treated with EtOH (EtOH; 4.5 g/kg, 25%) or calorie-matched quantities of maltose/dextrin (M/D) throughout gestation. Water diffusion and tissue microstructure were investigated using DTI (fractional anisotropy, FA) and histology (anisotropy index, AI), respectively. Both FA and AI decreased with age, and were higher in the EtOH than the M/D group at postnatal ages (P)0, P3, and P6. Additionally, there was a significant correlation between FA and AI measurements. These findings provide evidence that disruptions in cerebral cortical development induced by EtOH exposure can be revealed by water diffusion anisotropy patterns, and that these disruptions are directly related to cerebral cortical differentiation.

1. Introduction

Fetal alcohol spectrum disorders (FASDs) are the leading cause of environmentally related birth defects and mental retardation in the western world (Moore and Ganglier 2010),

*Correspondence to: Christopher D. Kroenke, PhD, Advanced Imaging Research Center, Mail Code: L452, Oregon Health & Science University, 3181 SW Sam Jackson Park Road, Portland, OR 97239-3098, kroenkec@ohsu.edu, Phone: (503) 418-1569, Fax: (503) 418-1543.

affecting between an estimated 0.6 and 4.5 of every 1,000 live births in the United States (Centers for Disease Control and Prevention). Individuals with FASD suffer from neurological deficits, including impairments in cognitive ability and behavioral control (Guerri et al. 2009). While current criteria for diagnosis of FASD are reliable, present diagnoses predominantly occur in mid to late childhood (Elliot et al. 2008, Streissguth et al. 2004). Due to the potential to use magnetic resonance imaging (MRI) technology non-invasively in vivo, MRI research has been applied to the study of cerebral cortical development in FASD in order to identify new biomarkers that can be used to facilitate early diagnostic and treatment strategies (Astley et al. 2009, Godin et al. 2010, Leigland et al. 2013, Nardelli et al. 2011, O'Leary-Moore et al. 2010, Parnell et al. 2009, Sowell et al. 2001, 2008, Yang et al. 2011, Zhou et al. 2011). Structural imaging in humans has been performed in children and adolescents affected by FASD, revealing decreased brain volume, cerebral cortical volume and abnormal cerebral cortical thickness caused by prenatal exposure to alcohol (Astley et al. 2009, Nardelli et al. 2011, Sowell et al. 2001, 2008, Yang et al. 2011, Zhou et al. 2011). Additionally, animal studies focused on earlier developmental time points have demonstrated reduced brain and cerebral cortical volume, reduced cerebral cortical thickness, and reduced cerebral cortical surface area resulting from prenatal ethanol (EtOH) exposure at time periods that correspond to late gestation and early postnatal periods in humans (Godin et al. 2010, Leigland et al. 2013, O'Leary-Moore et al. 2010, Parnell et al. 2009).

Thus far, most imaging research into early cerebral cortical development in FASD has focused on macrostructural developmental abnormalities such as brain size and shape (Astley et al. 2009, Godin et al. 2010, Leigland et al. 2013, Nardelli et al. 2011, O'Leary-Moore et al. 2010, Parnell et al. 2009, Sowell et al. 2001, 2008, Yang et al. 2011, Zhou et al. 2011). However, histological studies have also reported cellular-level anomalies in early cerebral cortical development caused by prenatal exposure to EtOH (Cui et al. 2010, Davies and Smith 1981, Fabregues et al. 1985, Hammer and Scheibel 1981, Stoltenburg-Didinger and Spohr 1983, Yanni and Lindsley 2000). Specifically, in rodent studies of the effects of fetal EtOH exposure, atypical cellular morphology has been observed in the developing cerebral cortex that potentially contributes to cognitive and behavioral problems associated with FASD (Cui et al. 2010, Davies and Smith 1981, Fabregues et al. 1985, Hammer and Scheibel 1981, Stoltenburg-Didinger and Spohr 1983, Yanni and Lindsley 2000). Diffusion tensor imaging (DTI) non-invasively provides information about the morphological complexity of microanatomical structures in the brain through measurements of the directional dependence of water diffusion, reflected in the parameter fractional anisotropy (FA) (see Mori and Zhang 2006 for review). Given the sensitivity of DTI to microstructural properties of tissue, we have set out to determine whether this neuroimaging modality has the potential to detect FASD at early phases of central nervous system development.

A number of recent studies have demonstrated that diffusion MRI measurements are sufficiently sensitive to detect perturbations to normal cerebral cortical cellular morphology including those induced in response to perinatal hypoxia-ischemia in the rat (Sizonenko et al. 2007) and sheep (Dean et al. 2013), gliosis in response to traumatic brain injury in the rat (Budde et al. 2011) and visual sensory deprivation in the form of neonatal enucleation in the ferret (Bock et al. 2010). In order to facilitate the ability to interpret diffusion MRI measurements in terms of tissue properties related to neuron morphology, recent efforts have lead to the development of strategies to directly quantify the orientation distribution of axonal and dendritic processes using images obtained by light microscopy (Budde and Frank 2012, Jespersen et al. 2012, Leergard et al. 2010). However, it remains to be tested whether diffusion MRI can be used to detect abnormal cortical development in FASD, and whether differences in diffusion measurements between brains of control and fetal-EtOH-exposed individuals can be related to aberrant microstructural properties of the cerebral cortex.

Herein, DTI measurements of water diffusion anisotropy were used to investigate effects of prenatal exposure to EtOH on early cerebral cortical development in a previously described rat model of FASD (Leigland et al. 2013), and were also compared with histological measurements reflecting tissue microstructure (Budde and Frank 2012). The research presented here shows that abnormal neuronal differentiation caused by prenatal exposure to EtOH, specifically a disruption in the formation and development of neuronal processes such as axons and dendrites in the developing cerebral cortex, can be detected by DTI in experimental versus control animals at ages corresponding to late gestation in humans.

2. Methods

2.1 Animal Care

Long-Evans rats were purchased from Harlan Laboratories (Livermore, CA), and were delivered to the Department of Comparative Medicine at Oregon Health & Science University. Virgin female dams (N=7) were ages 9 – 10 weeks and body masses were approximately 200 – 224 g. Proven breeder males (N=4) were ages 14 – 15 weeks, and body masses were approximately 325 – 349 g. All animals received standard chow, and participated in approximately one week of handling before experimental procedures began.

Breeding procedures are the same as those published previously (Leigland et al. 2013). Pregnant dams were assigned to one of two treatment groups: EtOH-treated (EtOH; n=4) or Maltose/Dextrin-treated (M/D; n=3). Alcohol and maltose/dextrin administration, as well as blood EtOH concentration collection procedures were the same as those previously published.

All possible measures were taken to minimize animal pain or discomfort. All experiments were carried out in accordance with the NIH "*Guide for the Care and Use of Laboratory Animals"* (NIH publication no. 86-23, revised 1987) and were approved by the OHSU animal care and use committee.

2.2 Tissue Collection

At 3 postnatal time points (P0, P3, P6), pups from the dams were sacrificed, and their brains collected for analysis (n = 3–4/age/group; a total of 22 pups from 7 litters). Pups were given an i.p. injection of approximately 0.5 mL euthasol (Butler-Schein Animal Health Supply, Dublin, OH). Heparin (0.01 mL/10 mL), with phosphate buffered saline (1x PBS), was injected into the left cardiac ventricle until the fluid of the right cardiac atrium was clear. Phosphate-buffered paraformaldehyde (PFA; 2%, approximately 40 mL) was then injected into the left cardiac ventricle. The brains were extracted and placed in PFA (2%, approximately 40 mL) for 24 hours. Samples were then transferred to 1X PBS at 4°C. During the course of this study it was found that FA is systematically lower in brain tissue exposed to alkaline pH than in non-alkaline exposed tissue (Leigland et al. in preparation). To remove PFA alkalinity as a possible confound, all tissue underwent a step in which it was incubated for 24 hrs in pH 11 phosphate buffer. After at least 48 hours in 1X PBS at 4°C, olfactory bulbs were removed from the brains at the lateral olfactory tract, and remaining spinal cord was severed between the C1 dorsal root of the spinal cord and the medulla. Left and right hemispheres were separated, and right hemispheres of each brain were utilized for all subsequent procedures (a subset of the hemispheres were used in previously described experiments presented in Leigland et al. 2013).

2.3 MRI procedures

Hemispheres were placed in a modified 3 mL syringe filled with 1X PBS, and allowed to equilibrate to room temperature. Samples were placed into a one-turn solenoid RF coil

manufactured in the laboratory (transmit/receive, tuned and matched to 500MHz), and the entire apparatus was placed in the isocenter of an 11.7 Tesla magnet (Bruker, Germany) interfaced with a 9 cm inner-diameter magnetic field gradient coil insert (maximum gradient strength of 70 G/cm per x, y and z axis).

A multi-slice spin-echo pulse sequence incorporating a Stejskal-Tanner diffusion sensitization gradient pair was used to acquire DTI data. Axial slices, 200 μm thick, of the entire hemisphere were imaged (TR = 4000 – 5000, TE = 42.7 ms, FOV = 5.20 × 1.28 cm, Matrix = 250 × 64, Voxel size = $(0.2\ mm)^3$, Averages=6, Scan time = 12 hours). The diffusion weighting factor (b value) was 2500 s/mm^2 with a gradient duration and separation of δ = 12 ms and Δ = 21 ms, respectively. Two scans were acquired in which b=0, and diffusion anisotropy was measured using a 25-direction, icosahedral sampling scheme as described previously (Jespersen et al. 2012, Kroenke et al. 2009). Scanning time was approximately 12 hours total per sample.

2.4 DTI analyses

FA and apparent diffusion coefficient (ADC) maps were generated from DTI data using software provided by Bruker (Bruker, Rheinstetten, Germany). Additionally, maps of axial and radial diffusivity were made using the eigenvalues of the diffusion tensor (λ_1 or $\lambda_{\parallel}$ and $(\lambda_2 + \lambda_3)/2$ or $\lambda_{\top}$, respectively). FA images were transferred into ITK-SNAP (Yushkevich et al. 2006) where $\lambda_{\top}$ whole brain masks were created by removing the cerebellar area from individual images. Three dimensional masks of the entire isocortex were delineated on the FA parametric maps for each hemisphere using ITK-SNAP software (Yushkevich et al. 2006). For visualization purposes, cerebral cortical FA was projected onto mid-cortical surfaces constructed using the CARET software package (Van Essen et al. 2001, www.brainvis.wustl.edu/caret, St. Louis, MO) for one EtOH and one M/D hemisphere at each age examined (Figure 1). At each surface node, mean FA for all isocortical voxels within a 9 voxel cube $(1.8\ mm)^3$ centered on the node was projected onto the surface. The Figure 1 insets illustrate the positions of the isocortical mask and mid-cortical surfaces for the E and M/D hemisphere. The isocortex/allocortex boundary was defined laterally by the rhinal fissure, and rostrally by the lateral olfactory tract. Only data from the isocortex was used for analysis, as allocortical regions do not undergo the same sequence of cellular differentiation throughout development as the isocortex (Sidman and Rakic1973, 1982), and thus the allocortex has diminished FA relative to other cortical regions (Kroenke et al. 2007, 2009). The medial boundary of the isocortex was identified at the junction with the corpus callosum. Isocortical masks were made individually for each subject, taking care not to include white matter. Brain and isocortical volumes were calculated based on the number of voxels in the whole brain and isocortical masks, respectively. The voxel number was multiplied by the volume of one voxel $(0.2\ mm)^3$ and multiplied by 2 so as to represent total brain and total isocortical volumes (as opposed to hemispheric volumes). Mean FA, ADC, axial diffusivity and radial diffusivity values over the entire isocortex were calculated. Volume and FA values were calculated in Matlab (Matlab, The Mathworks, Boston, MA). Directional FA maps were created to view the primary orientation of water diffusion obtained via DTI.

2.5 Histological methods

Subsequent to DTI scanning, hemispheres were sectioned coronally on a vibratome at a thickness of 200 μm. One rostral-coronal, one mid-coronal (half-way between the rostral and caudal extent of the brain) and one caudal-coronal section per subject were chosen for histological processing. Slices were dehydrated in increasing concentrations of EtOH (25%, 50%, 75%, 100%), then submerged in DiI (DiI[1,1′-Dioctadecyl-3,3,3′,3′-tetramethylindocarbocyanine; Anaspec) stain (0.25 mg/mL EtOH) for approximately 3

minutes. Coronal slices were then rehydrated by reversing the order of EtOH concentrations used for dehydration. Sections were mounted on slides using Prolong Antifade Gold mounting medium (Invitrogen, Molecular Probes). Virtual slices of slides were obtained with the MBF Bioscience StereoInvestigator using an Apochomat 10X objective (Morphology and Imaging Core, Oregon National Primate Research Center), and individual 10X images were then combined to make a montage of the entire tissue slice using Stereoinvestigator software (MBF Bioscience, Williston, VT). Histological measures of anisotropy were derived from fluorescent whole-slice images according to the procedure described by Budde and Frank (Budde and Frank 2012). A measure of in-plane anisotropy (anisotropy index, AI) was determined using structure tensor analysis to obtain AI maps at a resolution of $(0.74\ \mu m)^2$. In brief, the structure tensor is a second-order symmetric positive matrix that describes the dominant direction of the gradient of staining intensity within a local neighborhood of each pixel. The AI is calculated using the eigenvalues of the structure tensor, and is a measure of tissue microstructure analogous to FA that ranges from 0 (no anisotropy) to 1 (extreme anisotropy), and describes anisotropy in the the local structure of stained elements. Analogous to the directional FA maps, the primary orientation of fibers obtained by structure tensor analysis in the AI maps was color coded according to a red (medial-lateral) and green (dorsal-ventral) color scheme. Masks of the isocortex were manually drawn on individual AI maps, and mean AI values over this area were calculated.

2.6 Histology and DTI comparisons

A subset of subjects and slices were included in histological analyses and comparisons (subject n = 1 – 3/age/group, slice n = 3 – 8/age/group with 1 – 3 each of rostral-, mid- and caudal-coronal slices). In order to directly compare FA and AI values, mean isocortical FA values from the slices in the FA maps corresponding to the histological images were collected. Additionally, directional FA and AI maps were created to compare the orientation distribution of neuronal processes in similar slices. Considering the AI maps capture only in-plane structure, the directional FA maps depict only the in-plane components of the diffusion tensor for direct comparison (Figure 3).

2.7 Statistics

Unpaired t-tests were utilized to examine possible body mass differences between EtOH and M/D dams. A two-way ANOVA (analysis of variance) model was used to determine effects of the independent variables, treatment group (EtOH and M/D) and age group (P0, P3, P6), on dependent variables: brain volume, isocortical volume, FA, ADC, axial diffusivity and radial diffusivity and AI. Upon determining interaction effects between group and age, post-hoc unpaired t-tests were used to determine separate effects of age and/or group on the dependent variables. Correlation analyses were used to examine the relationship between FA and AI. Uncorrected alpha was set at p=0.05 for all analyses. Statistics were implemented in Statview [SAS, Cary, NC]).

3. Results

3.1 EtOH Administration and Macrostrucutral Outcomes

As observed in earlier studies using this EtOH administration procedure (Leigland et al. 2013), mean maternal mass values at the beginning and end of the 20-day period, in which gavages were administered, did not differ significantly between treatment groups, nor did the body masses gained throughout pregnancy. Additionally, the EtOH dosing procedure resulted in blood EtOH concentrations in excess of the standard threshold for intoxication in humans (> 0.8 mg/ml) over a period extending more than 3 hours per day (data not shown).

To compare the effects of fetal EtOH exposure on macroscopic and microstructural properties of brain tissue, structural image analyses were performed to ensure that the previously-observed reductions in brain size resulting from EtOH exposure were also observed here. For 14 of the 22 hemispheres examined in this study, the cerebral cortical thickness of the opposite brain hemisphere was characterized in previously published work (Leigland et al. 2013). Consistent with the earlier report, brain volume and isocortical volume increased significantly with age (brain volume: $F_{2,16}$=183, p<0.0001, isocortical volume: $F_{2,16}$=168, p<0.001). Additionally, both brain and isocortical volumes were higher in the M/D group and lower in the EtOH group (brain volume: $F_{1,16}$=21.8, p<0.001, isocortical volume: $F_{1,16}$=20.4, p<0.001) (Figure 2 A and B). Mean brain volume for the EtOH group was 0.285 cm^3, which was 27.9% lower than the mean for the M/D group, 0.340 cm^3. Mean isocortical volume for the EtOH group was 0.112 cm^3, or 18.8% lower than the mean for the M/D group, 0.138 cm^3. Differences in brain sizes are illustrated for two typical brains from each treatment group at each age in Figure 1. There was no significant interaction between age and treatment groups for either brain or isocortical volume (brain volume: $F_{2,16}$=2.12, p=0.15, isocortical volume: $F_{2,16}$=2.91, p=0.08). These data suggest that prenatal EtOH exposure results in decreased brain and isocortical volumes at early postnatal time points in the rat, a time that corresponds to the second half of gestation of human central nervous system development.

3.2 Microstructural Outcomes

In order to characterize microstructural features of EtOH-exposed brains potentially associated with the observed brain volume reductions, DTI and histological measurements were compared between EtOH and M/D groups. Consistent with other DTI-based studies of rat cerebral cortical development (Bockhorst et al. 2008, Huang et al. 2008, Sizonenko et al. 2007), isocortical FA decreased significantly with age over the P0 to P6 range in both treatment groups ($F_{2,16}$=117, p<0.0001). Further, isocortical FA and was found to be higher in the EtOH group than the M/D group at all ages ($F_{1,16}$=24.1, p<0.001). Mean FA for the EtOH group was 0.204, which was 12.7 % higher than the mean for the M/D group, 0.178. There was no interaction between age and treatment group ($F_{2,16}$=3.36, p=0.06) (Figure 2 C). Coronal views of FA parameter maps shown in Figure 1 illustrate the differences in isocortical FA observed between EtOH and M/D hemispheres obtained from P3 rats. As can be seen in the lateral views of cortical surfaces, FA differences are not localized to a single area, but are spread throughout the entire cerebral cortex. Additionally, as visible in the raw FA images in Figure 1, higher FA is most clearly seen in the superficial layers of the cortex in the EtOH versus M/D subject. Thus, throughout the age range spanning P0 to P6, isocortical FA is increased in EtOH animals relative to age-matched M/D controls.

ADC, as well as axial and radial diffusivities were investigated to help interpret any age group or treatment group effects on FA during development. ADC was found to increase with age ($F_{2,16}$=4.20, p<0.05), but was not significantly different between treatment groups ($F_{1,16}$=3.64, p=0.07), and there was no interaction between factors ($F_{2,16}$=2.34, p = 0.13). There were no age group or treatment group effects on axial diffusivity (age: $F_{2,16}$=0.445, p=0.65 treatment: $F_{1,16}$=1.03, p=0.33), and no interaction between factors ($F_{2,16}$=2.35, p=0.13). Interestingly, radial diffusivity was found to increase with age ($F_{2,16}$=11.23, p<0.001) and was lower in the EtOH than the M/D group ($F_{1,16}$=5.38, p<0.05). No interaction was found between factors in regard to radial diffusivity ($F_{2,16}$=2.28, p=0.13). Thus, increased FA observed in EtOH brains appears to be mediated by reduced radial diffusivity.

It was also of interest to determine whether DTI could detect an effect of prenatal EtOH exposure on white matter maturation during the P0 – P6 time period. To address this, an exploratory analysis of differences in FA in white matter was conducted. Regions of interest

(ROI) were drawn within the corpus callosum of each subject, and mean FA within these ROIs was determined. FA was not significantly different between treatment groups ($F_{1,16}$=2.46, p=0.14) or among age groups ($F_{2,16}$=0.442, p=0.65), and no statistical interaction was found ($F_{2,16}$=0.724, p=0.50).

For a subset of the hemispheres examined by DTI, the tissue was subsequently processed and analyzed with histological methods. Figure 3 shows an FA map (left), a 2D directional FA map (center), and a 2D directional AI map (right) for a mid-coronal slice of a hemisphere obtained from a P6 M/D rat. In the 2D directional maps, the magnitudes of the diffusion tensor and histological structure tensor components parallel to the dorsal/ventral axis are encoded by green color, and parallel to the medial/lateral axis are encoded by the red color (note that while blue coloring is typically used to represent water diffusion anisotropy oriented in the dorsal – ventral plane (e.g. Huang et al. 2008), green coloring was substituted here to increase contrast for visualization purposes). Throughout the coronal slice, a high degree of similarity is observable, indicating close agreement in the orientation of the measures derived from diffusion imaging and light microscopy.

Further comparisons between FA and AI measurements were performed by analyzing the effects of age and fetal EtOH exposure on AI. As shown in Figure 2D, AI exhibited patterns that exactly paralleled the patterns observed for isocortical FA. Specifically, AI decreased significantly with age ($F_{2,25}$=44.4, p<0.0001), AI was higher in the EtOH than in the M/D group ($F_{1,25}$=6.36, p<0.05), and there was no significant interaction between age and treatment group ($F_{2,25}$=1.07, p=0.36). Mean AI for the EtOH group was 0.208, which was 13.5 % higher than the mean for the M/D group, 0.180. In order to further refine the comparison between FA and AI, ANOVA was repeated for isocortical FA in the same tissue in which light microscopy data was available. As expected, this analysis revealed the same statistically significant effects [isocortical FA decreased significantly with age ($F_{2,25}$=45.7, p<0.0001), FA was higher in the EtOH than in the M/D group ($F_{1,25}$=5.80, p<0.05), and there was no significant interaction between age group and treatment group ($F_{2,25}$=0.991, p=0.39)].

Last, a correlation analysis was conducted to compare AI and FA values from the same tissue areas in the same subjects. There was a significant overall correlation between FA and AI (R=0.861, p<0.0001, Figure 4). This correlation indicates that FA is reflective of AI, and suggests that FA measurements are sufficiently sensitive to detect abnormal properties of tissue microstructure caused by prenatal exposure to EtOH.

4. Discussion

We have used a rat model of FASD to demonstrate that fetal exposure to EtOH (4.5 g/kg/day of 25% EtOH throughout 20 days of gestation) disrupts subsequent early postnatal morphological differentiation of the cerebral cortex in a manner that results in abnormally elevated water diffusion anisotropy relative to cerebral cortices of age-matched control animals. Previous work has shown that EtOH exposure during early cerebral cortical development results in cell number reductions (Burke et al. 2009, Dunty et al. 2001), abnormal cerebral cortical microscopic organization (e.g. Granato 2006, Margret et al. 2005) and dendritic abnormalities (Cui et al. 2010, Davies and Smith 1981, Fabregues et al. 1985, Hammer and Scheibel 1981, Stoltenburg-Didinger and Spohr 1983, Yanni and Lindsley 2000). Therefore, in this study, we aimed to produce rats with similar perturbations to cerebral cortical development, to test the hypothesis that such effects could be detected with diffusion MRI. In the early developing cerebral cortex, FA measurements in the isocortical gray matter begin high and decrease with age concurrently with the differentiation of neurons (Leigland and Kroenke 2011). Disrupted development in the form of fewer and

shorter dendritic branches would allow for fewer pathways, parallel to the pial surface, along which water can diffuse. We therefore reasoned that FA would be higher as a consequence of disrupted development of cellular processes. The direction of the observed effect, in which cerebral cortical FA is higher in EtOH animals compared to M/D controls, indicates the morphological complexity of axonal and dendritic processes is lower in EtOH treated animals. This is in accordance with past literature that has shown dendritic abnormalities in response to pre- and perinatal exposure to EtOH in animals at time points similar to those studied here (Cui et al. 2010, Davies and Smith 1981, Fabregues et al. 1985, Hammer and Scheibel 1981, Stoltenburg-Didinger and Spohr 1983, Yanni and Lindsley 2000). These findings were confirmed in the current study by performing a direct comparison of tissue characterized by MRI and structure tensor analysis (Budde and Frank 2012) of light microscopy images.

In an investigation of ADC, axial and radial diffusivities, an increase in ADC with age was found. While some human studies of early development note a general decrease in ADC with age (Huppi et al. 1998, Neil et al. 1998), one human study looking at development before to gestational week 30 found an increase in ADC prior to a steady decline similar to that found in previous studies (McKinstry et al. 2002). Specifically, McKinstry and co-workers found an increase in ADC during gestational weeks 26 through 32, which corresponds to approximately P3 through P5 in the rat (Workman et al. 2013). Not all studies are in agreement regarding ADC patterns in the cerebral cortex during this time period, with one study in the rat showing constant mean diffusivity from P0 – P8 (Bockhorst et al. 2008), and another showing a decrease in the rat from P3 – P6 (Sizonenko et al. 2007). However, an increase in ADC very early on in development has been explained by McKinstry and colleagues (McKinstry et al. 2002) as potentially reflecting programmed cell death in the cerebral cortex. The lack of treatment group differences in ADC suggests that the biological mechanisms underlying this phernomenon are not affected by prenatal exposure to ethanol.

Interestingly, in the present experiment, axial diffusivity remained constant while radial diffusivity increased with age. Again, there does not appear to be any consensus among previous studies regarding axial or radial diffusivity patterns. At time points similar to those studied here, rodent studies either confirm no change in axial diffusivity within the cerebral cortex (Larvaron et al. 2007), or report reductions in axial diffusivity with maturation (Bockhorst et al. 2008, Calabrese and Johnson 2013, Huang et al. 2008). Regarding radial diffusivity, either increases similar to those seen here are reported (Bockhorst et al. 2008, Calabrese and Johnson 2013), or no change in radial diffusivity is reported (Huang et al. 2008, Larvaron et al. 2007). Considering a loss of FA during early cortical development, an increase in radial diffusivity corresponds to an increase in complexity of dendritic arbors seen with maturation over this time period (Leigland and Kroenke 2011). Of note, the significantly lower radial diffusivity values in the EtOH compared to the M/D group may correspond to fewer or shorter collateral dendritic arbors seen in FASD (as discussed above). This lends further support to the theory that there is disrupted isocortical development seen with prenatal ethanol exposure detectable by FA measurements.

Interestingly, no differences in white matter ROIs within the corpus callosum were found during this age period. Previous research suggests that there may be increases in white matter FA at time periods immediately after those investigated here in normally-developing rats (e.g. Calabrese and Johnson 2013). However, from P0 to P6, FA in the cerebral cortex appears to be more sensitive to the deleterious effects of EtOH exposure on brain development than FA within white matter. In the future, studies may benefit from investigating both gray and white matter structures, as they provide important independent

information that reflects distinct neurodevelopmental events throughout maturation of the central nervous system.

Previously, we have found that fetal EtOH exposure is associated with reduced cerebral cortical volume, both as a consequence of reduced cerebral cortical surface area and thickness, throughout postnatal development (Leigland et al. 2013). Such findings are consistent with results from studies of human subjects affected by FASD, in which fetal EtOH exposure is associated with subsequently reduced cerebral cortical volume and thickness (Zhou et al. 2011) (but see also Sowell et al. 2008, Yang et al. 2011, in which increased cortical thickness relative to total brain size in FASD individuals has also been observed). Cerebral cortical volumetric reductions were also observed in the rats studied here. The link between cerebral cortical FA in the early postnatal rat brain and tissue microstructure therefore suggests that abnormalities in development of the neuropil and cerebral cortex differentiation may also underlie observed macroscopic volume differences between the treatment groups.

In the research presented here, alcohol was administered throughout gestation in the rat (corresponding to the first to middle-second trimester in humans), during which time neuronal generation, proliferation and migration take place. The effects of this insult were investigated during periods of rapid neuronal differentiation, corresponding to the early postnatal period in the rat and the late second trimester in humans. While immediate effects of alcohol administration have been demonstrated during cellular generation (Dunty et al. 2001), we observed that alcohol administration at this time also has consequences on the subsequent events relevant to the development of neural circuits, such as dendritic differentiation.

The lack of an observed interaction between the effects of treatment group and postnatal age on cerebral cortical FA and AI are consistent with our previous findings related to isocortical volume, which remained constant throughout adolescence and into adulthood. This suggests the microstructural differences observed with diffusion MRI may be persistent rather than transient with CNS development, and this is further supported by histological evidence of long-term effects of prenatal alcohol exposure on cell numbers in the rat (Chappel et al. 2007). However, as others have shown in rodents (Bockhorst et al. 2008, Huang et al. 2008, Larvaron et al. 2007, Mori et al. 2001, Sizonenko et al. 2007, see also Calabrese and Johnson 2013) and we and others have shown in other species (deIpolyi et al. 2005, Kroenke et al. 2007, 2009, McKinstry et al. 2002, reviewed in Leigland and Kroenke 2011) cerebral cortical FA decreases toward an asymptotically low value during the early postnatal period (corresponding to the second half of gestation in humans; Leigland and Kroenke 2011). While FA is higher in EtOH animals throughout the time period studied here, an age-dependent reduction in FA is still observable in this group. Additionally, while two-way ANOVA failed to reveal an interaction between age and group, group differences do appear to decrease with age (e.g. compare FA differences at P0 to differences at P6 in Figure 2C). Cerebral cortical FA is expected to decay a further 33% of its range subsequent to P6, the latest time point examined herein, based on estimates derived from normally-developing rats (Olavarria et al. 2012). Thus, it may be possible that the treatment group differences shown here are transient. It may also be possible that at later ages, differences between treatment groups may not be detectable due to an inability to differentiate between low FA values. However, further research is necessary to definitively distinguish between permanent and transient effects of prenatal exposure to EtOH. Regardless, even if diffusion MRI-based investigation of the cerebral cortex is of limited utility at developmental periods that follow morphological maturation of the cerebral cortex and its associated reduction of water diffusion anisotropy, the data presented here strongly suggest this technique offers potential for early detection of neurodevelopmental sequelae of fetal EtOH exposure.

In quantitative anatomical studies of neuron morphology there are a number of outcomes that have been reported, including branch length, overall dendrite arbor length, branch order, radius and path distance from the soma (e.g. Donohue and Ascoli 2008). In general, such measurements are time consuming, because completely labeled neurons must be identified, and then comprehensively characterized. In this regard, an advantage of diffusion MRI compared to traditional anatomical techniques is the ease with which quantitative parameters reflecting morphological properties of ensembles of cells can be obtained, with the additional benefit of characterizing tissue microstructure in living subjects. In order to validate the proposed interpretation of diffusion MRI, specialized automated procedures have recently been developed for efficiently characterizing tissue microstructural peroperties related to cell morphology that are expected to be most closely related to diffusion MRI-based measurements, such as those measuring axonal and dendritic orientation distribution and AI (Budde and Frank 2012, Jespersen et al. 2012). For the current application, AI has been found to be a particularly robust measurement that can be used to characterize large areas of the cortex (or large numbers of dendrites), compared to methods requiring single dendrites. Although structure tensor analysis measures the overall morphology of tissues rather than isolated neurons and their processes, it provide an automated and quantitative measure of anisotropy that is directly analogous to measures of water diffusion anisotropy. These features have been used here to demonstrate correspondence between treatment-related differences in FA and characteristics of tissue microstructure.

5. Conclusion

This research identifies water diffusion anisotropy within the developing cerebral cortex as a measurement that is capable of detecting abnormal morphological differentiation resulting from fetal EtOH exposure. The proposed interpretation of the diffusion MRI results is supported by histological validational measurements, is consistent with previous animal model studies of other neurodevelopmental disorders, and therefore is supportive of our hypothesis that neuroimaging biomarkers focused on early cerebral cortical development are of value for detecting early anatomical signatures of fetal-EtOH-induced damage. Given the recent rapid pace of methodological advances to facilitate *in utero* MRI procedures, with specific emphasis on diffusion-based contrast (see Studholme 2011 for review) the findings presented here have potentially significant implications for the study of FASD in humans.

Acknowledgments

Support from NIH grants R01NS070022, R01AA021981, T32AA00746, T32AG023477, P30NS061800 and P50RR000163, and a grant from the Foundation for Alcohol Research is acknowledged. Data collected from the OHSU 12T MRI system is possible through support from The W.M. Keck Foundation.

References

1. Astley SJ, Aylward EH, Carmichael-Olson H, Kerns K, Brooks A, Coggins TE, Davies J, Dorn S, Gendler B, Jirikowic T, Kraegel P, Maravilla K, Richards T. Magnetic Resonance Imaging Outcomes From a Comprehensive Magnetic Resonance Study of Children With Fetal Alcohol Spectrum Disorders. Alcoholism: Clinical and Experimental Research. 2009; 33(10):1671–1689.
2. Bock AS, Olavarria JF, Leigland LA, Taber EN, Jespersen SN, Kroenke CD. Diffusion Tensor Imaging Detects Early Cerebral Cortex Abnormalities in Neuronal Architecture Induced by Bilateral Neonatal Enucleation: An Experimental Model in the Ferret. Frontiers in Systems Neuroscience. 2010; 4:1–11. [PubMed: 20204156]
3. Bockhorst KH, Narayana PA, Liu R, Ahobila-Vijjula P, Ramu J, Kamel M, Wosik J, Bockhorst T, Hahn H, Hasan KM, Perez-Polo JR. Early Postnatal Development of Rat Brain: In Vivo Diffusion Tensor Imaging. Journal of Neuroscience Research. 2008; 86:1520–1528. [PubMed: 18189320]

4. Budde MD, Frank JA. Examining Brain Microstructure Using Structure Tensor Analysis of Histological Sections. Neuro Image. 2012; 63(1):1–10. [PubMed: 22759994]
5. Budde MD, Janes L, Gold E, Turtzo LC, Frank JA. The Contribution of Gliosis to Diffusion Tensor Anisotropy and Tractography Following Traumatic Brain Injury: Validation in the Rat Using Fourier Analysis of Stained Tissue Sections. Brain. 2011; 134(Pt 8):2248–2260. [PubMed: 21764818]
6. Burke MW, Palmour RM, Ervin FR, Ptito M. Neuronal Reduction in Frontal Cortex of Primates After Prenatal Alcohol Exposure. Neuro Report. 2009; 20:13–17.
7. Calabrese E, Johnson GA. Diffusion Tensor Magnetic Resonance Histology Reveals Microstructural Changes in the Developing Rat Brain. Neuro Image. 201310.1016/j.neuroimage.203.01.101
8. Centers for Disease Control and Prevention. Fetal Alcohol Spectrum Disorders (FASDs): Data & Statistics. 2013. Available from: http://www.cdc.gov/NCBDDD/fasd/data.html
9. Chappell TD, Margret CP, Li CX, Waters RS. Long-Term Effects of Prenatal Alcohol Exposure on the Size of the Whisker Representation in Juvenile and Adult Rat Barrel Cortex. Alcohol. 2007; 41:239–251. [PubMed: 17630085]
10. Cui Z, Zhao K, Zhao H, Yu D, Niu Y, Zhang J, Deng J. Prenatal Alcohol Exposure Induces Long-Term Changes in Dendritic Spines and Synapsses in the Mouse Visual Cortex. Alcohol & Alcoholism. 2010; 45(4):312–319. [PubMed: 20543181]
11. Davies DL, Smith DE. A Golgi Study of Mouse Hippocampal CA1 Pyramidal Neurons Following Perinatal Ethanol Exposure. Neuroscience Letters. 1981; 26:49–54. [PubMed: 7290537]
12. Dean JM, McClendon E, Hansen K, Azimi-Zonooz A, Chen K, Riddle A, Gong X, Sharifnia E, Hagen M, Ahmed T, Leigland LA, Hohimer AR, Kroenke CD, Back SA. Prenatal Cerebral Ischemia Disrupts MRI-Defined Cortical Microstructure via Disturbances in Neuronal Arborization. Science Translational Medicine. 2013; 5(168):168ra7.
13. deIpolyi AR, Mukherjee P, Gill K, Henry RG, Partridge SC, Veeraraghavan S, Jin H, Lu Y, Miller SP, Ferriero DM, Vigneron DB, Barkovich AJ. Comparing Microstructural and Macrostructural Development of the Cerebral Cortex in Premature Newborns: Diffusion Tensor Imaging Versus Cortical Gyration. Neuro Image. 2005; 27:579–586. [PubMed: 15921934]
14. Donohue DE, Ascoli GA. A Comparative Computer Simulation of Dendritic Morphology. PLoS Computational Biology. 2008; 4(5):e1000089. [PubMed: 18483611]
15. Dunty WCJ, Chen S, Zucker RM, Dehart DB, Sulik KK. Selective Vulnerability of Embryonic Cell Populations to Ethanol-Induced Apoptosis: Implications for Alcohol-Related Birth Defects and Neurodevelopmental Disorder. Alcoholism: Clinical and Experimental Research. 2001; 25(10):1523–1535.
16. Elliott EJ, Payne J, Morris A, Haan E, Bower C. Fetal Alcohol Syndrome: A Prospective National Surveillance Study. Archives of Disease in Childhood. 2008; 93(9):732–737. [PubMed: 17704098]
17. Fabregues I, Ferrer I, Gairi JM, Cahuana A, Giner P. Effects of Prenatal Exposure to Ethanol on the Maturation of the Pyramidal Neurons in the Cerebral Cortex of the Guinea-Pig: A Quantitative Golgi Study. Neuropathology and Applied Neuobiology. 1985; 11:291–298.
18. Godin EA, O'Leary-Moore SK, Khan AA, Parnell SE, Ament JJ, Dehart DB, Johnson BW, Johnson GA, Styner MA, Sulik KK. Magnetic Resonance Microscopy Defines Ethanol-Induced Brain Abnormalities in Prenatal Mice: Effects of Acute Insult on Gestational Day 7. Alcoholism: Clinical and Experimental Research. 2010; 34(1):98–111.
19. Granato A. Altered Organization of Cortical Interneurons in Rats Exposed to Ethanol During Neonatal Life. Brain Research. 2006; 1069:23–30. [PubMed: 16386714]
20. Guerri C, Bazinet A, Riley EP. Foetal Alcohol Spectrum Disorders and Alterations in Brain and Behaviour. Alcohol and Alcoholism. 2009; 44:108–114. [PubMed: 19147799]
21. Hammer RP Jr, Scheibel AB. Morphologic Evidence For a Delay of Neuronal Maturation in Fetal Alcohol Exposure. Experimental Neurology. 1981; 74:587–596. [PubMed: 7297637]
22. Huang H, Yamamoto A, Hossain MA, Younes L, Mori S. Quantitative Cortical Mapping of Fractional Anisotropy in Developing Rat Brains. Journal of Neuroscience. 2008; 28:1427–1433. [PubMed: 18256263]

23. Huppi PS, Maier SE, Peled S, Zientara GP, Barnes PD, Jolesz FA, Volpe JJ. Microstructural Development of Human Newborn Cerebral White Matter Assessed In Vivo by Diffusion Tensor Magnetic Resonance Imaging. Pediatric Research. 1998; 44:584–590. [PubMed: 9773850]
24. Jespersen SN, Leigland LA, Cornea A, Kroenke CD. Determination of Axonal and Dendritic Orientation Distributions Within the Developing Cerebral Cortex by Diffusion Tensor Imaging. IEEE Transactions on Medical Imaging. 2012; 31:16–32. [PubMed: 21768045]
25. Kroenke CD, Taber EN, Leigland LA, Knutsen AK, Bayly PV. Regional Patterns of Cerebral Cortical Differentiation Determined By Diffusion Tensor MRI. Cerebral Cortex. 2009; 19:2916–2929. [PubMed: 19363145]
26. Kroenke CD, Van Essen DC, Inder TE, Rees S, Bretthorst GL, Neil JJ. Microstructural Changes of the Baboon Cerebral Cortex During Gestational Development Reflected in Magnetic Resonance Imaging Diffusion Anisotropy. Journal of Neuroscience. 2007; 27:12506–12515. [PubMed: 18003829]
27. Larvaron P, Boespflug-Tanguy O, Renou JP, Bonny JM. In Vivo Analysis of the Postnatal Development of Normal Mouse Brain by DTI. NMR in Biomedicine. 2007; 20:413–421. [PubMed: 17120295]
28. Leergard TB, White NS, de Crespigny A, Bolstad I, D'Arceuil H, Bjaalie JG, Dale AM. Quantitative Histological Validation of Diffusion MRI Fiber Orientation Distributions in the Rat Brain. PLoS One. 2010; 5(1):e8595. [PubMed: 20062822]
29. Leigland LA, Ford MM, Lerch JP, Kroenke CD. The Influence of Fetal Ethanol Exposure on Subsequent Development of the Cerebral Cortex as Revealed by Magnetic Resonance Imaging. Alcoholism: Clinical and Experimental Research. 201310.1111/acer.12051
30. Leigland, LA.; Kroenke, CD. A Comparative Analysis of Cellular Morphological Differentiation Within the Cerebral Cortex Using Diffusion Tensor Imaging. In: Raber, J., editor. Animal Models of Behavioral Analysis. Human Press c/o Springer Science; New York, NY: 2011. p. 329-251.
31. Margret CP, Li CX, Elberger AJ, Matta SG, Chappell TD, Waters RS. Prenatal Alcohol Exposure Alters the Size, But Not the Pattern, of the Whisker Representation in Neonatal Rat Barrel Cortex. Experimental Brain Research. 2005; 165:167–178.
32. McKinstry RC, Mathur A, Miller JP, Ozcan AO, Snyder AZ, Schefft GL, Almli CR, Shiran SI, Conturo TE, Neil JJ. Radial Organization of Developing Human Cerebral Cortex Revealed By Non-Invasive Water Diffusion Anisotropy MRI. Cerebral Cortex. 2002; 12:1237–1243. [PubMed: 12427675]
33. Moore, TE.; Gagnier, KR. Fetal Alcohol Syndrome. In: Weiner, IB.; Craighead, WE., editors. The Corsini Encyclopedia Psychology. Wiley; New York: 2010. p. 657-659.
34. Mori S, Itoh R, Zhang J, Kaufmann WE, van Zijl PC, Solaiyappan M, Yarowsky P. Diffusion Tensor Imaging of the Developing Mouse Brain. Magnetic Resonance in Medicine. 2001; 46:18–23. [PubMed: 11443706]
35. Mori S, Zhang J. Principles of Diffusion Tensor Imaging and its Applications to Basic Neuroscience Research. Neuron. 2006; 51:527–539. [PubMed: 16950152]
36. Nardelli A, Lebel C, Rasmussen C, Andrew G, Beaulieu C. Extensive Deep Gray Matter Volume Reductions in Children and Adolescents With Fetal Alcohol Spectrum Disorders. Alcoholism: Clinical and Experimental Research. 2011; 35(8):1404–1417.
37. National Institutes of Health. Guide for the Care and Use of Laboratory Animals. NIH Publication; 1987. p. 86-23.
38. Neil JJ, Shiran SI, McKinstry RC, Schefft GL, Snyder AZ, Almli CR, Akbudak E, Aronovitz JA, Miller JP, Lee BCP, Conturo TE. Normal Brain in Human Newborns: Apparent Diffusion Coefficient and Diffusion Anisotropy Measured by Using Diffusion Tensor MR Imaging. Radiology. 1998; 209:57–66. [PubMed: 9769812]
39. Olavarria JF, Bock AS, Leigland LA, Kroenke CD. Deafferentation-Induced Plasticity of Visual Callosal Connections: Predicting Critical Periods and Analyzing Cortical Abnormalities Using Diffusion Tensor Imaging. Neural Plasticity. 201210.1155/2012/250196
40. O'Leary-Moore SK, Parnell SE, Godin EA, Dehart DB, Ament JJ, Khan AA, Johnson GA, Styner MA, Sulik KK. Magnetic Resonance Microscopy-Based Analyses of the Brains of Normal and

Ethanol-Exposed Fetal Mice. Birth Defects Research Part A, Clinical and Molecular Teratology. 2010; 88(11):953–964.

41. Parnell SE, O'Leary-Moore SK, Godin EA, Dehart DB, Johnson BW, Johnson GA, Styner MA, Sulik KK. Magnetic Resonance Microscopy Defines Ethanol-Induced Brain Abnormalities in Prenatal Mice: Effects of Acute Insult on Gestational Day 8. Alcoholism: Clinical and Experimental Research. 2009; 33(6):1001–1011.
42. Sidman RL, Rakic P. Neuronal Migration, with Special Reference to Developing Human Brain: A review. Brain Research. 1973; 62:1–35. [PubMed: 4203033]
43. Sidman, RL.; Rakic, P. Development of the Human Central Nervous system. In: Haymaker, RDAW., editor. Histology and Histopathology of the Nervous System. C.C. Thomas; Springfield, IL: 1982. p. 3-145.
44. Sizonenko SV, Camm EJ, Garbow JR, Maier SE, Inder TE, Williams CE, Neil JJ, Huppi PS. Developmental Changes and Injury Induced Disruption of the Radial Organization of the Cortex in the Immature Rat Brain Revealed By In Vivo Diffusion Tensor MRI. Cerebral Cortex. 2007; 17:2609–2617. [PubMed: 17259644]
45. Sowell ER, Mattson SN, Kan E, Thompson PM, Riley EP, Toga AW. Abnormal Cortical Thickness and Brain-Behavior Correlation Patterns in Individuals With Heavy Prenatal Alcohol Exposure. Cerebral Cortex. 2008; 18(1):136–144. [PubMed: 17443018]
46. Sowell ER, Thompson PM, Mattson SN, Tessner KD, Jernigan TL, Riley EP, Toga AW. Voxel-Based Morphometric Analyses of the Brain in Children and Adolescents Prenatally Exposed to Alcohol. Cognitive Neuroscience and Neuropsychology. 2001; 12(35):515–523.
47. Stoltenburg-Didinger G, Spohr HL. Fetal Alcohol Syndrome and Mental Retardation: Spine Distribution of Pyramidal Cells in Prenatal Alcohol-Exposed Rat Cerebral Cortex; A Golgi Study. Developmental Brain Research. 1983; 11:119–123.
48. Streissguth AP, Bookstein FL, Barr HM, Sampson PD, O'Malley K, Young JK. Risk Factors for Adverse Life Outcomes in Fetal Alcohol Syndrome and Fetal Alcohol Effects. Developmental and Behavioral Pediatrics. 2004; 25(4):228–238.
49. Studholme C. Mapping Fetal Brain Development in utero Using MRI: The Big Bang of Brain Mapping. Annual Review of Biomedical Engineering. 2011; 13(1):345–368.
50. Van Essen DC, Dickson J, Harwell J, Hanlon D, Anderson CH, Drury HA. An Integrated Software System for Surface-Based Analysis of Cerebral Cortex. Journal of the American Medical Informatics Association. 2001; 41:1359–1378.
51. Workman AD, Charvet CJ, Clancy B, Darlington RB, Finlay BL. Modeline Transformations of Neurodevelopmental Sequences Across Mammalian Species. Journal of Neuroscience. 2013; 33:7368–7383. [PubMed: 23616543]
52. Yang Y, Roussotte F, Kan E, Sulik KK, Mattson SN, Riley EP, Jones KL, Adnams CM, May PA, O'Connor MJ, Narr KL, Sowell ER. Abnormal Cortical Thickness Alterations in Fetal Alcohol Spectrum Disorders and Their Relationships With Facial Dysmorphology. Cerebral Cortex. 2011:1–10.
53. Yanni PA, Lindsley TA. Ethanol Inhibits Development of Dendrites and Synapses in Rat Hippocampal Pyramidal Neuron Cultures. Developmental Brain Research. 2000; 120:233–243. [PubMed: 10775775]
54. Yushkevich PA, Piven J, Hazlett HC, Smith RG, Ho S, Gee JC, Gerig G. User-Guided 3D Active Contour Segmentation of Anatomical Structures: Significantly Improved Efficiency and Reliability. Neuro Image. 2006; 31(3):1116–1128. [PubMed: 16545965]
55. Zhou D, Lebel C, Lepage C, Rasmussen C, Evans A, Wyper K, Pei J, Andrew G, Massey A, Massey D, Beaulieu C. Developmental Cortical Thinning in Fetal Alcohol Spectrum Disorders. Neuro Image. 2011; 58:16–25. [PubMed: 21704711]

Highlights

- Ex vivo DTI was performed on fetal ethanol exposed and control rat pup brains
- Cerebral cortical diffusion anisotropy was higher in ethanol pups than controls
- Perturbed microstructure was confirmed with histological structure tensor analysis
- Diffusion MRI of the immature cerebral cortex offers promise as an FASD biomarker

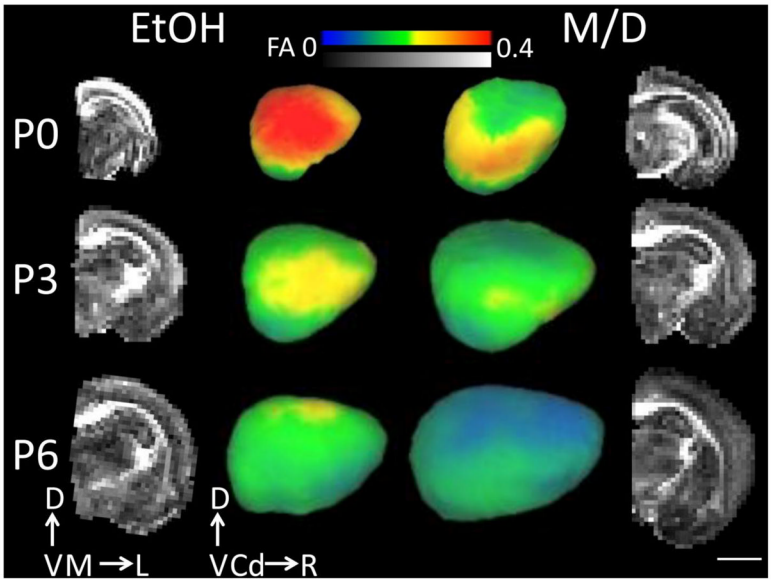

Figure 1.

The two middle columns of images are laterally-facing mid-cortical surface models of one rat postnatal day (P)0, P3 and P6 right hemisphere for each treatment group (ethanol (EtOH) and maltose/dextrin (M/D)), on which cortical FA at each mid-cortical surface node is projected. The outer columns represent mid-coronal FA maps for the right hemisphere of the same subjects depicted in the middle columns. Cortical FA decreased significantly with age. Additionally, cortical FA was largest, and isocortical volume smallest, in the EtOH group compared to the M/D group. This group difference is most visible in the outer layers of the cortex. Error bars represent one standard error. Scale bar is 4 mm. D = dorsal, V= ventral, M = medial, L= Lateral, Cd = Caudal, R = Rostral.

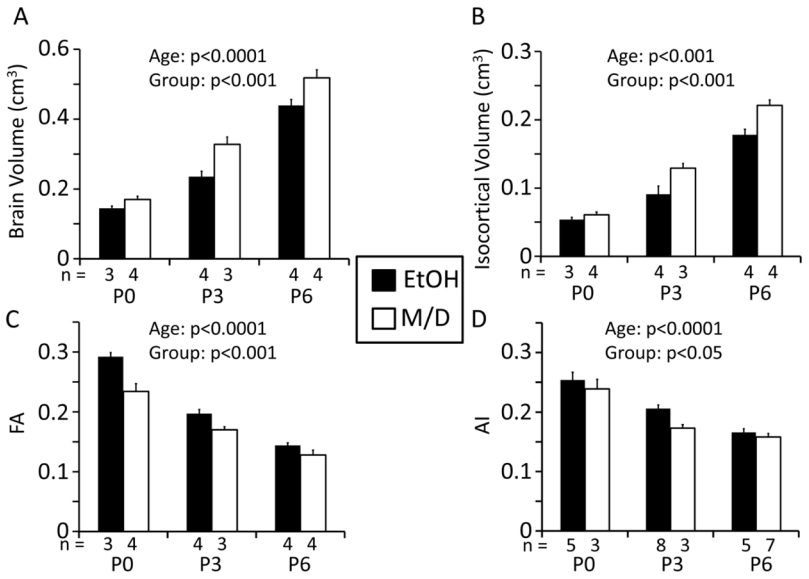

Figure 2.

A, B. Brain volume and isocortical volume in the rat (n = 3 – 4/age/group) increased significantly with age in both groups, and were both significantly lower in the EtOH than in the M/D group at all three ages [postnatal day (P)0, P3, P6]. C. Isocortical FA in both treatment groups decreased significantly with age. Additionally, across age groups, the maltose/dextrin (M/D) had the lowest mean isocortical FA, while the ethanol (EtOH) group had the highest FA. D. The anisotropy index (AI) for a subset of subjects (1–3/age/group), in both treatment groups decreased significantly with age. Additionally, across age groups, the maltose/dextrin (M/D) group had the lowest mean isocortical AI, while the ethanol (EtOH) group had the highest AI. Numbers of subjects in each group at each age are represented on the x-axes above the age group labels. Please note that for the brain volume, isocortical volume and FA analyses, numbers represent numbers of subjects. For the AI analysis numbers represent the numbers of histological slices included in the analysis. Statistical results for effects of age and group on each dependent variable are represented in each graph in the form of p-values.

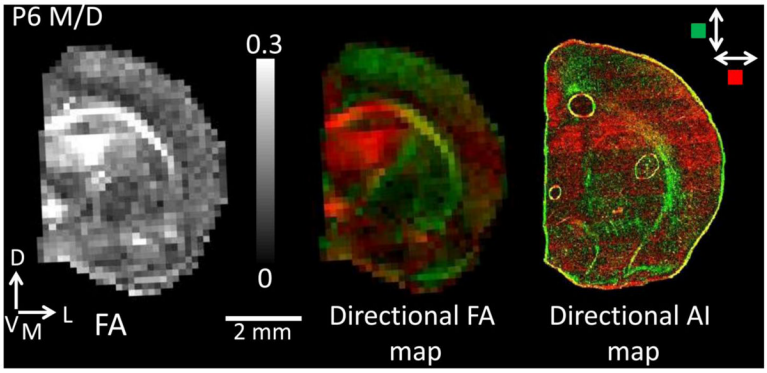

Figure 3.

An FA map for one P6 M/D subject is shown on the left corresponding to the directional FA map (center). The directional FA map is shown for the same section with only the in-plane orientation for direct comparison with the directional AI map (far right), which is necessarily constrained in two dimensions. Green color indicates tissues oriented in a dorsal-ventral direction, while red indicates a medial-lateral direction. Please note that while blue coloring is typically used to represent water diffusion anisotropy oriented in the dorsal – ventral plane (e.g. Huang et al. 2008), green coloring was substituted here to increase contrast for visualization purposes. There is a close correspondence between the directional FA and AI maps.

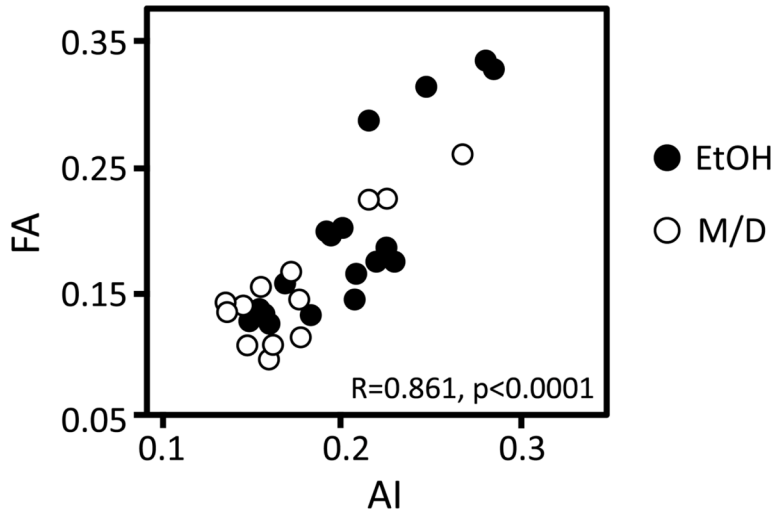

Figure 4.

A regression analysis investigating the relationship between AI and FA resulted in a significant direct overall association between AI and FA ($p < 0.001$). This relationship was also significant in both treatment groups separately (EtOH $p < 0.0001$, M/D $p < 0.0001$). This suggests that the morphological characteristics of neurons, represented by AI, underly FA meausurements in the developing cerebral cortex, and that this is true in both normal as well as FASD development.